Micromechanical Fatigue Modelling of the Size Effect in Micro-Scale 316L Stainless Steel Specimens

E. Donnelly, F. M. Weafer*, T. Connolley, P.E. McHugh, M. S. Bruzzi

College of Engineering and Informatics, National University of Ireland Galway, Ireland

*Corresponding author: Tel: (+353)-91-492723; E-mail: fiona.weafer@gmail.com

Received: 12 September 2017, Revised: 18 February 2019 and Accepted: 19 February 2019

DOI: 10.5185/amlett.2019.0012
www.vbripress.com/aml

Abstract

For many years, computational modelling and simulation studies have been used by developers to advance device design and have been reported in regulatory medical device submissions. However, cardiovascular stent materials in such computational models are typically assumed to behave as a continuum. This approach assumes that bulk material properties apply to the micro-sized structure, i.e. material behavior is scale independent. However, as size is reduced, mechanical size effects arise as the grain size to specimen width ratio drops below a critical value. These size effects cause material behavior to deviate significantly from bulk material behavior. If such a deviation in material behavior is to be captured within computational models, it is necessary to represent the crystalline structure of a metal and to capture the anisotropic behavior of individual grains within these models. This paper describes the development of such a modelling methodology to investigate the phenomenon of strain localization within grains of a 316L stainless steel specimen under fatigue loading conditions. Copyright © VBRI Press.

Keywords: Finite element, size effect, microstructure, 316L stainless steel, strain localization.

Introduction

Advances in micro-manufacturing techniques have allowed for the development of micro-sized components, devices and machines. Micro-scaled devices are designed for a range of applications, most notably in the biomedical stent device industry. These components are typically of a size scale such that factors which can largely be ignored at the macro-level can change the material behavior considerably at the micro-level. As size is reduced there is a corresponding reduction in the grain size to specimen width ratio, which subsequently induce mechanical size effects. Therefore, bulk material properties may no longer be sufficient to fully describe material behavior in micro-scaled components such as stents due to such size effects. For stainless steels, the critical value for which size effects take affect ranges typically from when there are 4-6 grains across the width [**1-6**]. To specifically examine the potential size effect on the fatigue characteristics of coronary stents materials, experimental examination of stents made from 316L stainless steel were completed by Weiss *et al.*, 2009 [**2**]. Such stents were expanded and cycled in a physiological solution for 50 million cycles at a frequency of 45 Hz. Post-expansion of the stents revealed regions of high deformation, with characteristic features such a slip lines on the surface, with apparent high dislocation densities near grain boundaries. It was observed that because of the small grain size/specimen size ratio, deformation behavior comparable to single crystal behavior occurred. Experimental work by the current authors also confirmed a size effect exists in the fatigue behavior of micro-scaled 316L stainless steel stent-like specimens. Test specimens investigated had a strut width of 50, 75, 100 and 150 µm with an average grain size of 10 ± 7µm. It was concluded that a size effect existed in the form of a reduced fatigue endurance limit of the smaller 50 µm specimens [**7**]. Due to the clear and detrimental impact of the size effect on device design and safety, it is necessary for continued investigation into this phenomenon.

The objective of this work is to establish if computational modelling can aid in the exploration of the main mechanisms involved in the mechanical size effect observed in the fatigue behavior of micro-scale 316L stainless steel components. Over the past three decades, a large class of research has been conducted to computationally link the grain level mechanical response to the response of a polycrystalline aggregate including developing a constrained hybrid model (Parks and Ahzi, 1990) [**8**], generalized Taylor models (Asaro, 1983; Asaro and Needleman, 1985; Mathur *et al.*, 1990; Kalidindi and Anand, 1992; Habraken and Duchene, 2004) [**9-13**] and Greens function fast Fourier transform (FFT) models (Lebensohn *et al.*, 2012; Eisenlohr *et al.*, 2013) [**14, 15**], constructing dislocation density-based crystal constitutive equations (Lee *et al.*, 2010) [**16**],

application of statistical continuum mechanics to study polycrystals (Garmestani *et al.*, 2001; Zhang *et al.*, 2011) [**17, 18**], and so on. A review paper by Roters *et al.*, 2010 [**19**] thoroughly evaluates continuum-based variational formulations for describing the elastic–plastic deformation of anisotropic heterogeneous crystalline matter. These approaches, commonly referred to as crystal plasticity finite-element models (CPFEM), are important both for basic microstructure-based mechanical predictions as well as for engineering design and performance simulations involving anisotropic materials. CPFEM has been used in simulations of strain heterogeneity at grain and sub-grain scale, which is associated with intrinsic size effect in polycrystalline metals Yalcinkaya *et al.*, 2017 [**20**], and in capturing the influence of loading orientations, sample textures and material's constants, such as hardening and strain rate sensitivity on the strain at which the plastic localization and surface roughening initiates (Zhao *et al.*, 2008; Zhang *et al.*, 2009; Iadicola *et al.*, 2012) [**21-23**] or shear band development (Inal *et al.*, 2002; Kuroda and Tvergaard, 2007; Lim *et al.*, 2014; Wu *et al.*, 2016) [**24-27**]. The general framework supplied by CPFEM formulations provides an attractive vehicle for developing a comprehensive theory of plasticity that incorporates existing knowledge of the physics of deformation processes into the computational tools of continuum mechanics with the aim of developing advanced and physically based design methods for engineering applications. In crystal plasticity theory, plastic flow is calculated in terms of continuum plastic shear strains on the individual slip systems, which are then summed across all the available slip systems to give the total deformation. As there are many hundreds of grains in even the simplest of strut models, such an approach, while potentially very accurate, is not suited to fatigue modelling in polycrystalline solids due to the excessive computational requirements imposed by such a model. To circumvent this issue, a method known as the 'microstructural-J2' method was developed. In this paper, applying this methodology, finite element models designed to approximately represent the structure and anisotropic material behavior of the grains were developed for a series of specimen sizes; specimens of widths of 14 µm, 19 µm, 28 µm, 75 µm, and 150 µm were examined. These models aim to shed further light on the potential size effect in micro-scale 316L stainless steel specimens, particularly focusing on the process of strain localization.

Finite element modelling

Finite element model design

The numerical models developed in this paper are designed to approximately represent the microstructure of a 316L stainless steel experimental stent-like specimen. As shown in **Fig. 1(a)**, the grains and grain boundaries are clearly visible in a polished and etched sample of 316L stainless steel. The strut in this image is traversed by six, approximately equi-axed, grains giving a grain size to specimen width ratio of 6. Such grains are represented in the models by an idealized, hexagonal grain geometry as illustrated in **Fig. 1(b)**. A series of 2-D struts of length 500 µm, with varying aspect ratios were created. The aspect ratio was changed by increasing the strut width through the addition of more through-thickness grains (i.e. keeping the grain size constant). Ten models were created for each series of specimen sizes, namely, a 14 µm, 19 µm, 28 µm, 75 µm series and a symmetric boundary applied to the 75 µm model to represent a 150 µm series while still taking account of the Poisson's ratio effect. The strut geometries were completed by adding half hexagons to the upper and lower surfaces. The 2-D finite element mesh was generated with pre-processing/finite element software MSC Patran 2003. For additional accuracy a through-thickness component of constraint was afforded to the 2-D structure using 8-noded quadrilateral CPEG8R generalised plane strain elements. Completed input files were then processed and post-processed by ABAQUS® V 6.5 on a 24 CPU super computer.

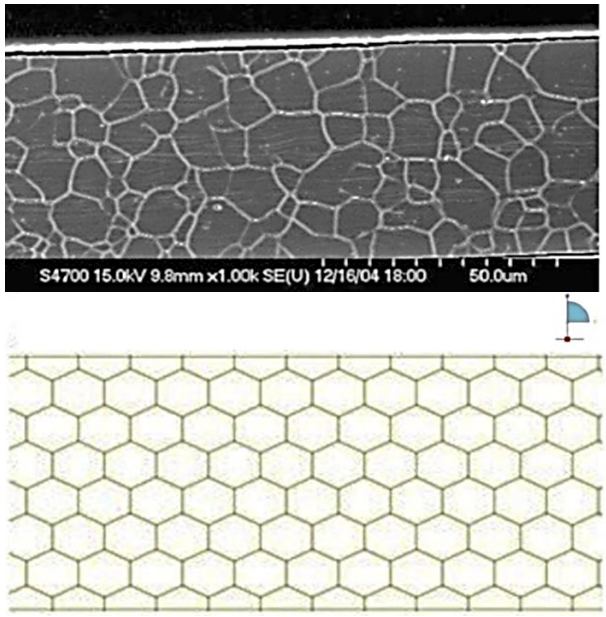

Fig. 1. (a) Micrograph of a polished and etched sample of 316L stainless steel (courtesy Helen Cuddy, NCBES, NUI Galway) and (b) section of strut model showing both the geometry and the arrangement of the hexagonal grains.

Cyclic loading of the strut was simulated by constraining the left-hand surface of the model in the horizontal (x-axis) direction while a negative pressure load (450 MPa tensile stress) was applied to the right-hand surface, also in the horizontal direction. Sinusoidal cyclic loading, with an load ratio (R-ratio) of 0.1, was applied to the models utilizing the *AMPLITUDE command [**28**] which allows variable loading patterns to be prescribed using a Fourier series as follows:

$$F(x) = 0.55 + 0.45Sin(x) \quad (1)$$

Rigid body motion was prevented by constraining the node at the bottom left-hand corner in both the horizontal and the vertical (y-axis) direction. The bottom

right-hand corner node was also constrained in the vertical direction. This was necessary to prevent buckling from occurring for the low width struts, high aspect ratio struts (e.g. an aspect of 35:1 exists in the case of the 14µm strut). Symmetry boundary conditions were applied to the 75µm series of models, in order to increase the apparent width to 150µm, in the form of an additional boundary condition on the bottom surface of the model constraining motion in the vertical direction. Given the experimental loading profile, where an initially high strain amplitude is followed by potentially millions of applications of cycles of a lower strain amplitude, it was hypothesized that the microstructural conditions that lead ultimately to fatigue failure and hence to the size effect, would be established very early on in the life of the fatigue test. During finite element simulation of a fatigue test, the maximum load is achieved on the first cycle. Differences in plastic strain levels within grains will therefore be evident at the end of this initial cycle. A small number of additional cycles are required to establish if the rate of strain accumulation after the first cycle is greater for grains with initially higher strain levels, therefore each model was subjected to 20 loading cycles during the finite element simulations.

Modelling methodology

Microstructural – J2 (M-J2) modelling methodology

The Microstructural-J2 (M-J2) modelling method seeks to combine the relevant elements of crystal plasticity (i.e. its ability to describe single grain behavior) with the computational efficiency of continuum mechanics. This can be achieved by assigning to each grain in the strut its own material property derived from the mechanical behavior of a single crystal with its dependence on its orientation with respect to the global loading direction [**29**]. In this paper, this calibration is achieved by using the crystal plasticity method to generate stress-strain curves for all possible loading orientations of a single anisotropic grain subjected to a standard load. This approach resulted in a selection of 43 unique stress-strain curves, representing the behavior of each grain with respect to its orientation to the loading direction. These curves were then randomly assigned to the grains within the ten strut models for each specimen size series using a random number generator [**30**]. While a significant element of accuracy is sacrificed with the M-J2 method, the general behavior of a polycrystalline material can be described. As the grains behave in a pre-determined manner, influenced only by the level of constraint and applied load, solution times are much faster than for an equivalent model incorporating the crystal plasticity constitutive behavior.

It must be stated that the purpose of the modelling work in this paper is not to develop a fatigue failure predictive capability but rather to elucidate the strain localization mechanisms involved in the experimentally observed size effect. Simulations were performed for 20 loading cycles only, and while material property data was generated by a crystal plasticity model of face centre cubic 316L stainless steel, the data was not calibrated against actual test specimens. No damage mechanisms other than plasticity were incorporated into the models and, consequently, no failure mechanisms are represented. While the modelling methodology adopted in this paper is limited in its applicability, it is sufficient to describe the evolution of plastic strain within the first few cycles. Such is the nature of a high cycle fatigue test, in that, differences in strain localization which become apparent at such an early stage will undoubtedly result in, or contribute significantly to, failure of the test specimen.

Hardening curves

In this study, the Bauschinger effect [**31, 32**] provides an explanation for the lowering of yield stress on reverse loading of a specimen that was previously plastically deformed in the opposite loading direction. A hardening model capable of describing this effect is necessary to model the accumulation of plastic strain that accompanies cyclic loading (and leads ultimately to fatigue crack initiation and growth). Therefore, a simple linear kinematic hardening model was adopted in this work as the hardening model. This constitutive model, though rather basic and limited in its range of application, is sufficient to describe the accumulation of plastic strain in the initial stages of a fatigue test (cycles 1 – 20). In this study, the Bauschinger effect is described by allowing the yield surface to translate in the direction of loading. An increment of plastic strain will occur if the maximum stress in the cycle is sufficient to raise the yield point for reverse loading above the minimum stress in the fatigue cycle. Plastic strain accumulation with the linear kinematic hardening model is therefore reliant upon concordant values of the load ratio (R-ratio), maximum stress and yield point. The 43 different linear hardening curves are displayed in **Fig. 2**. One of the major limitations of the linear kinematic hardening method is that within the plastic regime, the material will continue to deform infinitely. This is unrealistic, however, and limits the range of application of the method to a small number of cycles beginning with a state of zero plasticity.

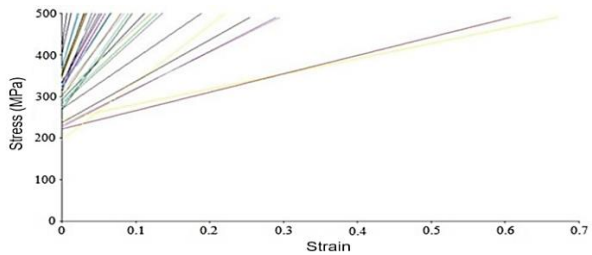

Fig. 2. Hardening curves for 43 different crystal orientations used in this study.

Results and discussion

Equivalent plastic strain (PEEQ) contour plots

A total of 20 loading cycles, at a common R-ratio and maximum stress, were applied to the various strut

models; namely, 14 µm, 19 µm, 28 µm, 75 µm and 150 µm strut width sizes. The equivalent plastic strain (PEEQ) contour plots of 14 µm and 150 µm models (Fig. 3) reveal a difference between the relatively small and large struts, with the smaller struts appearing to undergo a more localized trend of PEEQ accumulation. This difference in simulated behavior can be attributed to a reduction in constraint experienced by the thinner models. As the grain size to specimen width ratio is reduced, the mechanical behavior of individual grains assumes a greater role in determining the behavior of the entire strut. From this work it can be concluded that it is not the orientation of a single grain that is of importance, rather the orientation of a group of neighbouring grains that combine to create a 'soft region'. In a situation of reduced constraint, when this soft region is loaded to a level sufficient to cause plastic deformation, localization of plastic strain will occur within this region. It is proposed that the wider strut contains sufficient numbers of grains to ensure that homogeneous material behavior is approximated and dominates over the more localized inhomogeneous material behavior **Fig. 3(a)**. Reducing the strut width subsequently reduces the level of constraint experienced by regions within the strut **Fig. 3(b)**. Softer regions will be exposed as the grain size to specimen width ratio is reduced. Without the reinforcing effect of the harder grain network, strain distribution becomes increasingly inhomogeneous, with the consequent localization of strain within softer bands of grains occurring in the narrower specimens (as seen in **Fig. 3(b)**).

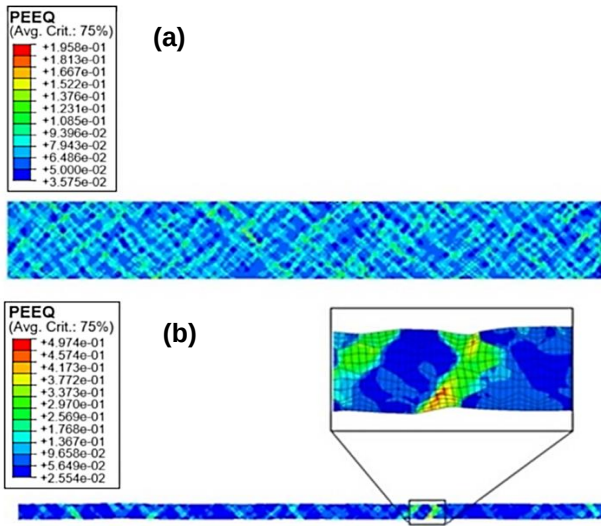

Fig. 3. Contour plots of equivalent plastic strain (PEEQ) for struts with (a) 14 µm, and (b) 150 µm width.

History plot of equivalent plastic strain (PEEQ) accumulation

As mentioned, from the equivalent plastic strain (PEEQ) contour plots following loading of the samples computationally, it is proposed that PEEQ localization occurs in the narrower strut models. The validity of this observation was investigated by selecting grains of a particular orientation in each of the five models and outputting the PEEQ accumulation history of these grains. Utilizing this, an average value for each series was subsequently calculated (as illustrated in **Fig. 4**). Clear differences between struts of different widths can be identified, with narrower struts having higher levels of PEEQ accumulation than wider struts. More specifically, the differences indicate that for a given stress, the magnitude of PEEQ within grains is dependent upon the size of the strut relative to the size of the grain (the specimen width to grain size ratio). In conclusion, the process of strain localization occurring as a result of cyclic loading, as identified initially by the contour plots of PEEQ, has been confirmed as being a size dependent effect. Relative to the wider strut series, the 14 µm and 19 µm series struts accumulate higher levels of average PEEQ, have higher maximum PEEQ values, greater range of PEEQ values and greater standard deviation within the values under conditions of cyclic loading (Fig. 4). On the other hand, the relatively wider 28 µm, 75 µm and 150 µm struts behave in a manner akin to that of a bulk material; a lower range of PEEQ values, with lower levels of scatter, within grains indicates uniformity of plastic strain accumulation. In addition, the total elongation and apparent surface roughness of the narrow struts was found to be greater than that of the wider struts in the finite element models. This trend can also be attributed to conditions of reduced constraint due to a reduction in specimen width and consequent reduction in the strut width to grain size ratio. In conclusion, the narrower samples (14 µm and 19 µm) experience higher average levels of PEEQ, combined with the irregular distribution of plastic strain within grains, suggesting strongly that strain localization is taking place.

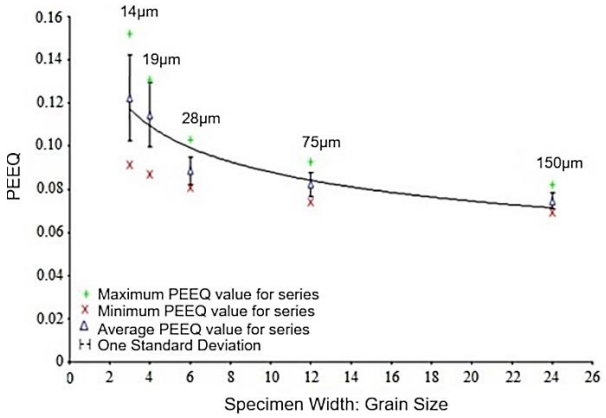

Fig. 4. Average equivalent plastic strain (PEEQ) accumulation for strut series and associated specimen width to grain size ratio with trend line.

Concluding remarks

Finite element models representing a range of strut thicknesses, namely 14 µm, 19 µm, 28 µm, 75 µm and 150 µm were used to elucidate the mechanisms that contribute to size-dependent material behavior; in particular, fatigue damage initiation in the form of strain localization. The strut specimens were modelled using an

idealized crystalline structure, thus describing in a simple manner the inhomogeneous nature of strain distribution. A small number of cyclic loads at a common load ratio (R-ratio) and maximum stress were applied to the various strut models. A size effect was found to occur within a few cycles of fatigue loading in the thinner struts in a manner which would, in reality, likely lead to a longer term accumulation of localized plastic strain and fatigue damage with an overall reduction in the fatigue performance of such components. It was found that the mechanical behavior of narrower struts is entirely dependent upon the orientation and arrangement of its constituent grains. In addition, the statistics of plastic strain magnitude distributions in the smaller strut specimens have higher mean values and higher standard deviations than in larger struts. Therefore, the narrower the strut the greater the influence a softer region will have, and consequently, the more random its material behavior. These results suggest that statistical methods may offer assistance in the design and reliability of very small stents.

In the future scope of this work, experimental fatigue testing on a range of suitable 316L specimens are to be completed. From the results of this paper, it would be expected that a size effect will be evident in the fatigue performance of smaller specimens. In order to experimentally determine the cause of this size effect, the outer surfaces and fracture surfaces of failed test specimens will be examined using scanning electron microscopy (SEM). These SEM studies may collaborate and thus strengthen the results presented in this paper by providing evidence that the process of strain localization is indeed occurring and is most pronounced in the smaller specimens. The surface roughness of the test specimens will also be measured in order to further confirm SEM observations using white light interferometry.

In summary, it was found there occurs a higher general level of deformation within the thinner samples in addition to a greater degree of strain localization, higher maximum and lower minimum values of plastic strain, higher levels of total deformation, higher incremental strain accumulation values and higher levels of surface roughness. It is a combination of these factors that may lead to a reduction in fatigue life of such components as early crack initiation would be more probable with a quicker propagation rate under load control cyclic loading. In conclusion, under conditions of fatigue loading, the finite element models employed in this paper suggest that the material behavior of thin struts differs from that of the wider struts, due to a size effect, in a manner which is likely to result in a decrease in the fatigue life of the thin specimens.

Acknowledgements

This study was funded by Enterprise Ireland as part of the Development of Software for Small Scale Implanted Metallic Structures (DESIMS) research programme.

Author's contributions

Conceived the plan: E.D., M.S.B; Performed the expeirments: E.D.; Data analysis: E.D., M.S.B, T.C., P.E.McH, F.M.W; Wrote the paper: F.W.W. Authors have no competing financial interests.

References

1. Wiersma, S.; Taylor, D.; *Fatigue and Fracture of Engineering Materials and Structures*, **2005**, *28*, 1153.
2 Weiss, S.; Meissner, A.; Fischer, A.; *Journal of the Mechanical Behaviour of Biomedical Materials*, **2009**, *2*, 210.
3. Murphy, B.P.; Savage, P.; McHugh, P.E.; Quinn, D.F.; *Annals of Biomedical Engineering*, **2003**, *31*, 686.
4. Connolley, T.; McHugh, P.E.; Bruzzi. M.; *Fatigue and Fracture of Engineering Materials and Structures*, **2005**, *28*, 1119.
5. Wharry, J.P.; Yano, K.H.; Patki, P.V.; *Scripta Materialia*, **2019,** *162*, 63.
6. Gao, S.; Bai, Y.; Zheng, R.; Tian, Y.; Mao, W.; Shibata, A.; Tsuji, N.; *Scripta Materialia*, **2019**, *159*, 28.
7. Donnelly, E.; Weafer, F.M.; Connolley, T.; McHugh, P.E.; Bruzzi, M.S.; *International Journal of Fatigue*, **2017**, *95*, 1.
8. Parks, D.; Ahzi, S.; *Journal of the Mechanics and Physics of Solids*, **1990**, *38*, 701.
9. Asaro, R.; *Advances in Applied Mechanics*, **1983**, *23*, 1.
10. Asaro, R.; Needleman, A.; *Acta Metallurgica*, **1985**, *33*, 923.
11. Mathur, K.K.; Dawson, P.R.; Kocks, U.; *Mechanics of Materials*, **1990**, *10*, 183.
12. Kalidindi, S.; Anand, L.; *International Journal of Mechanical Sciences*, **1992**, *34*, 309.
13. Habraken, A.M.; Duchene, L.; *International Journal of Plasticity*, **2004**, *20*, 1525.
14. Lebensohn, R.A.; Kanjarla, A.K.; Eisenlohr, P.; *International Journal of Plasticity*, **2012**, *3233*, 59.
15. Eisenlohr, P.; Diehl, M.; Lebensohn, R.; Roters, F.; *International Journal of Plasticity*, **2013**, *46*, 37.
16. Lee, M.; Lim, H.; Adams, B.; Hirth, J.; Wagoner, R.; *International Journal of Plasticity*, **2010**, *26*, 925.
17. Garmestani, H.; Lin, S.; Adams, B.; Ahzi, S.; *Journal of the Mechanics and Physics of Solids*, **2001**, *49*, 589.
18. Zhang, L.; Dingreville, R.; Bartel, T.; Lusk, M.T.; *International Journal of Plasticity*, **2011**, *27*, 1432.
19. Roters, F.; Eisenlohr, P.; Hantcherli, L.; Tjahianto, D.D.; Bieler, T.R.; Raabe, D.; *Acta Materialia*, **2010**, *58*, 1152.
20. Yalcinkaya, T.; Demircia, A.; Simonovski, I.; Ozdemir, I.; *Procedia Engineering*, **2017**, *207*, 998.
21. Zhao, Z.; Ramesh, M.; Raabe, D.; Cuitino, A.M.; Radovitzky, R.; *International Journal of Plasticity*, **2008**, *24*, 2278.
22. Zhang, F.; Bower, A.F.; Mishra, R.K.; Boyle, K.P.; *International Journal of Plasticity*, **2009**, *25*, 49.
23. Iadicola, M.A.; Hu, L.; Rollett, A.D.; Foecke, T.; *International Journal of Solids and Structures*, **2012**, *49*, 3507.
24. Inal, K.; Wu, P.D.; Neale, K.W.; *International Journal of Solids and Structures*, **2002**, *39*, 983.
25. Kuroda, M.; Tvergaard, V.; *International Journal of Plasticity*, **2007**, *23*, 244.
26. Wu, Y.; Shen, Y.; Wu, P.; Chen, K.; Yu, Y.; *International Journal of Solids and Structures*, **2016**, *96*, 265.
27. Lim, H.; Carroll, J.; Battaile, C.C.; Buchheit, T.E.; Boyce, B.; Weinberger, C.R.; *International Journal of Plasticity*, **2014**, *60*, 1.
28. ABAQUS Analysis User's manual V6.5, ABAQUS Inc., Dassault Systemes, Providence, RI, USA, **2009.**
29. Weafer F.M.; Guo Y.; Bruzzi M.S.; *Journal of the Mechanical Behavior of Biomedical Materials*, **2016**, *53*, 210.
30. A C-program for MT19937: Coded by Takuji Nishimura, considering the suggestions by Topher Cooper and Marc Rieffel, Copyright Makoto Matsumoto and Takuji Nishimura, **1997**.
31. Dieter, G.E.; Mechanical Metallurgy, 2nd Edition, Published by McGraw-Hill, New York, USA, **1976**.
32. Suresh, S.; Fatigue of Materials, 2nd Edition, Published by Cambridge University Press, Cambridge, UK, **1998**.

